

# Collaborative Merging of Radio SLAM Maps in View of Crowd-sourced Data Acquisition and Big Data

Kenneth Batstone<sup>a</sup>, Magnus Oskarsson and Kalle Åstrom<sup>b</sup>

*Centre of Mathematical Sciences, Lund University, Sölvegatan 18A, 222 10 Lund, Sweden*

**Keywords:** Toa Self-calibration, Crowdsourced, Big Data, Radio Slam.

**Abstract:** Indoor localization and navigation is a much researched and difficult problem. The best solutions, usually use expensive specialized equipment and/or prior calibration of some form. To the average person with smart or Internet-Of-Things devices, these solutions are not feasible, particularly in large scales. With hardware advancements making Ultra-Wideband devices more accurate and low powered, this unlocks the potential of having such devices in commonplace around factories and homes, enabling an alternative method of navigation. Therefore, indoor anchor calibration becomes a key problem in order to implement these devices efficiently and effectively. In this paper, we present a method to fuse radio SLAM (also known as Time-Of-Arrival self-calibration) maps together in a linear way. In doing so we are then able to collaboratively calibrate the anchor positions in 3D to native precision of the devices. Furthermore, we introduce an automatic scheme to determine which of the maps are best to use to further improve the anchor calibration and its robustness but also show which maps could be discarded. Additionally, when a map is fused in a linear way, it is a very computationally cheap process and produces a reasonable map which is required to push for crowd-sourced data acquisition.

## 1 INTRODUCTION

Navigation has become a key part of modern civilisation, with most people using systems such as GPS on a daily basis, in their cars or on their person, integrated into their smart phones. The demand for positioning systems is also increasing with the era of 5G upon us. With 5G, we expect to see an increase of positioning accuracy in addition to having more devices, such as Internet-Of-Things (IoT), to also required positioning. For example, items in warehouses will require positioning to enable automation in the warehouses to improve efficiency.


Currently GPS provides good positioning for most users in an outdoor environment. Unfortunately, this cannot be said once inside a building. Once inside, the GPS signals are heavily attenuated, meaning the accuracy of the positioning can decrease to encompass a whole build or more. When this occurs users must use an alternative system to navigate indoors.


There are currently many options to overcome this problem but they all come with their own draw-

backs. In robotics, many use optical devices to perform SLAM (Simultaneous localization and mapping, (Durrant-Whyte and Bailey, 2006)) such as cameras and LIDAR, which produce good results but such devices can be expensive and computationally tasking. This restricts such methods to small environments with a low amount of dynamic features. For mobile phone users, a large focus has been using the signal strength of Wi-Fi networks to perform positioning since the infrastructure currently exists in most buildings but due to the nature of radio signals in complex environments, they have a low accuracy and with distance, the errors increase exponentially, (Li et al., ).

One such technology which is commercially available is Ultra-Wideband (UWB). These devices are low powered and perform 2-way timing in order to obtain high precision in positioning, between two devices. This unlocks the potential of having such devices in common place around factories and homes, enabling an alternative method of navigation indoors for people and Internet of Things (IoT) devices.

Another technology which shows promise is round-trip time (RTT) being enabled on Wi-Fi. With RTT, it is expected to perform ranging between routers and mobile device with as low as 1 metre ac-

<sup>a</sup>  <https://orcid.org/0000-0001-8328-1052>

<sup>b</sup>  <https://orcid.org/0000-0002-8689-7810>

curacy. Many modern routers have the ability to perform this but currently awaits a firmware update. This technology uses the 802.11mc IEEE standard, which has been enabled on Android Pie devices. A strong advantage to this option is that the infrastructure already exists.

With these developments comes further issues. Due to the large number of devices, calibration of the anchors becomes problematic. Currently large datasets require vast amounts of memory and processing power, which is impossible for most machines. In this paper we present new research on methods for large scale anchor self-calibration problem. Here we present a method to merge maps together in a linear way. In doing so we build a library of tools in order to determine the quality of each map and then to be able to fuse them together to produce a global map. Additionally, when a map is merged in such a way, it is a relatively computationally cheap process and produces a reasonable map which is required to push for crowd-sourced data acquisition. The proposed method will help bridge the memory requirement issues and the ability to select the best datasets.

The proposed method was tested on both simulated and real UWB distance measurements. These datasets are created using 2-way timing, therefore it is a Time-Of-Arrival (TOA) self-calibration problem.

The TOA self-calibration problem, is the problem of determining the positions of a number of receivers and transmitters given only receiver-transmitter distances. Here, there is no prior knowledge of the anchor positions.

## 2 BACKGROUND

To solve such problems, one method is to solve a minimal case and extend that solution. Minimal cases for low rank matrix factorization, for missing data, were investigated in (Jiang et al., 2015). In (Batstone et al., 2016) a RANSAC paradigm was used in conjunction with minimal solvers and explored in order to obtain a robust and fast solution of the TOA self-calibration problem, with missing data and noise. In (Batstone et al., 2017) a sequential merging scheme was created to explore the potential of real-time anchor calibration. One pitfall of the described scheme was that as more data was collected, memory requirements and computational complexity increased which limited the system.

The TOA self-calibration problem and other indoor SLAM methods are rarely performed in large scale using radio. Computer vision research has address some issues common to both optical SLAM and

TOA self-calibration problem, such as memory limits, accuracy and computational power. In (Byröd and Åström, 2009) and (Byröd and Åström, 2010), the authors exploit the structure of the Jacobian so that memory limits and computational complexity are improved to allow for SLAM in larger environments with acceptable losses in accuracy.

In (Puyol et al., 2013), a solution was given for large scale SLAM, with promising memory requirements, computational effort and an accuracy of  $0.5m$  in 2D, but this works differs since the authors use foot mounted inertial measurement units (IMU) to crowd-source SLAM maps, which is not as prevalent as radio infrastructure. In (Chanier et al., 2008) map fusion was explored for a multi-robot SLAM framework, but this method was tested on only two maps. More research has been conducted in this area, (Schmuck and Chli, 2017; Liu et al., 2016), but still very few robots and maps are used when merging. In (Van Opendenbosch et al., 2018), the authors address the issue of large memory requirements needed for Collaborative Visual SLAM. Although optical SLAM and TOA self-calibration share similar solutions to similar problems, they differ greatly in accuracy and the type of data. In optical SLAM many other instruments on the robot assist the formation of the solution and improves the accuracy. This provides a rich and reliable dataset. For the TOA self-calibration using radio systems, it is common that there are fewer anchor positions than user sender positions. This means that when merging anchor positions, the sparsity of the data is a constraint on the solution and prone to errors due to the accuracy of the ranging.

## 3 METHOD

We will now describe the basic underlying geometry of our problem. Let  $\mathbf{R}_i$ ,  $i = 1, \dots, m$  and  $\mathbf{S}_j$ ,  $j = 1, \dots, n$  be the spatial coordinates of  $m$  receivers (e.g. Ultra-Wideband anchors) and  $n$  transmitters (e.g. Crazyflie quadcopter), respectively. For measured time of arrival  $t_{ij}$  from transmitter  $\mathbf{R}_i$  and receiver  $\mathbf{S}_j$ , we have  $vt_{ij} = \|\mathbf{R}_i - \mathbf{S}_j\|_2$  where  $v$  is the speed of measured signals and  $\|\cdot\|_2$  is the  $l^2$ -norm. The speed  $v$  is assumed to be known and constant. We further assume that we, at each receiver can distinguish which transmitter  $j$  each event is originating from. This can be done e.g. if the signals are temporally separated or using different frequencies. We will in the following work with the distance measurements  $d_{ij} = vt_{ij}$ . It is quite common that such data contains both missing data from poor signal communications and outliers due to inaccuracies of the hardware measurements.

The TOA calibration problem can then be defined as follows,

**Problem 1.** (Time-of-Arrival Self-Calibration) Given absolute distance measurements

$$d_{ij} = \|\mathbf{R}_i - \mathbf{S}_j\|_2 + \varepsilon_{i,j}, \quad (1)$$

where the receiver positions are defined as  $\mathbf{R}_i$ ,  $i = 1, \dots, m$  and transmitter positions as  $\mathbf{S}_j$ ,  $j = 1, \dots, n$ . Here the errors  $\varepsilon_{i,j}$  are assumed to be either **inliers**, in which case the errors are small ( $\varepsilon_{i,j} \in N(0, \sigma)$ ) or **outliers**, in which case the measurements are way off.

Here we will use the set  $W$  for the indices  $(i, j)$  corresponding to the inlier measurements.

The Time-of-Arrival Self-Calibration problem can be solved by computing the bundle adjustment of (2), shown below.

$$\min_{\mathbf{R}, \mathbf{S}} \sum_{(i,j) \in W} (d_{i,j} - \|\mathbf{R}_i - \mathbf{S}_j\|_2)^2. \quad (2)$$

For simplification, (2) can be represented as,

$$\operatorname{argmin} \sum |d - f(\mathbf{R}, \mathbf{S})|^2 \quad (3)$$

where  $f(\mathbf{R}, \mathbf{S}) = \|\mathbf{R} - \mathbf{S}\|_2$  can be the nonlinear function for all combinations of  $\mathbf{R}, \mathbf{S}$ . Therefore it can be assumed that there exists an optimal  $\mathbf{R}^*$  and  $\mathbf{S}^*$ , such that  $a_{opt}$  is the minima, ie.

$$a_{opt} = \sum |d - f(\mathbf{R}^*, \mathbf{S}^*)|^2. \quad (4)$$

Then the sum of the residuals can be linearized around  $\mathbf{R}^*$  and  $\mathbf{S}^*$  as

$$a(\mathbf{R}, \mathbf{S}) \approx a_{opt} + J \begin{bmatrix} \mathbf{R} - \mathbf{R}^* \\ \mathbf{S} - \mathbf{S}^* \end{bmatrix}, \quad (5)$$

where  $J$  is the jacobian of  $f$  wrt.  $\mathbf{R}$  and  $\mathbf{S}$ . The problem can be reformulated as

$$a(\mathbf{R}, \mathbf{S}) \approx a_{opt} + [J_{\mathbf{R}} \quad J_{\mathbf{S}}] \begin{bmatrix} \Delta \mathbf{R} \\ \Delta \mathbf{S} \end{bmatrix}. \quad (6)$$

We can include the contribution of  $\mathbf{S}$  into the expression by solving

$$\min_{\Delta \mathbf{S}} |a_{opt} + J_{\mathbf{R}} \Delta \mathbf{R} + J_{\mathbf{S}} \Delta \mathbf{S}|^2 \quad (7)$$

which has the closed form solution  $\Delta \mathbf{S} = -(J_{\mathbf{S}}^T J_{\mathbf{S}})^{-1} J_{\mathbf{S}}^T J_{\mathbf{R}} \Delta \mathbf{R}$  where  $^T$  denotes matrix transpose. Insertion into (6) yields

$$a(\mathbf{R}, \mathbf{S}) \approx a_{opt} + (I - J_{\mathbf{S}}(J_{\mathbf{S}}^T J_{\mathbf{S}})^{-1} J_{\mathbf{S}}^T) J_{\mathbf{R}} \Delta \mathbf{R}, \quad (8)$$

where  $I$  denotes the identity matrix of proper size. In order to reduce the amount of data being saved in a database, a matrix  $A$  is introduced such that

$$A = (I - J_{\mathbf{S}}(J_{\mathbf{S}}^T J_{\mathbf{S}})^{-1} J_{\mathbf{S}}^T) J_{\mathbf{R}}. \quad (9)$$

Now  $A$  above can be decomposed into  $A = VU$  where  $U$  is a upper triangular matrix and  $V$  is a unitary matrix. Hence,

$$\begin{aligned} |a(\mathbf{R}, \mathbf{S})|^2 &= |V^T a(\mathbf{R}, \mathbf{S})|^2 \approx |V^T a_{opt} + U \Delta \mathbf{R}|^2 \\ &= |a_{opt}|^2 + |U \Delta \mathbf{R}|^2. \end{aligned} \quad (10)$$

If two such solutions are available, then the sum of the norms can be formulated as

$$\begin{aligned} |a_1(\mathbf{R}, \mathbf{S})|^2 + |a_2(\mathbf{R}, \mathbf{S})|^2 &\approx |a_{1,opt}|^2 + \dots \\ &\dots + |U_1(\mathbf{R} - \mathbf{R}^*_{1})|^2 + |a_{2,opt}|^2 + |U_2(\mathbf{R} - \mathbf{R}^*_{2})|^2. \end{aligned} \quad (11)$$

This expression can be minimized for  $R$  as

$$\mathbf{R}_{opt} = (U_1^T U_1 + U_2^T U_2)^{-1} (U_1^T U_1 \mathbf{R}^*_{1} + U_2^T U_2 \mathbf{R}^*_{2}). \quad (12)$$

Which has the general expression, for  $k$  maps as,

$$\begin{aligned} \mathbf{R}_{opt} &= (U_1^T U_1 + U_2^T U_2 + \dots + U_k^T U_k)^{-1} \\ &\quad (U_1^T U_1 \mathbf{R}^*_{1} + U_2^T U_2 \mathbf{R}^*_{2} + \dots + U_k^T U_k \mathbf{R}^*_{k}). \end{aligned} \quad (13)$$

Since in reality, some of the calculated maps will be erroneous due to the environment in which the measurements are taken, a weighting term is therefore introduced, where  $\lambda_k \in [0, 1]$ .

$$\begin{aligned} \mathbf{R}_{opt}(\lambda) &= (\lambda_1^2 U_1^T U_1 + \lambda_2^2 U_2^T U_2 + \dots + \lambda_k^2 U_k^T U_k)^{-1} \\ &\quad (\lambda_1^2 U_1^T U_1 \mathbf{R}^*_{1} + \lambda_2^2 U_2^T U_2 \mathbf{R}^*_{2} + \dots + \lambda_k^2 U_k^T U_k \mathbf{R}^*_{k}). \end{aligned} \quad (14)$$

In order to solve for the problem in (14), a new variant of the objective function for the full bundle adjustment (2) is used. Here, one only needs to solve for the vector  $\lambda = [\lambda_1, \dots, \lambda_k]$  as shown in (15),

$$\min_{\lambda} \sum_k \sum_{(i_k, j_k) \in W_k} (\lambda_k (d_{i_k, j_k} - \|\mathbf{R}_{opt_{i_k}}(\lambda) - \mathbf{S}_{j_k}\|_2))^2. \quad (15)$$

This, therefore, can be seen as a relaxation of (2), where the  $\lambda$  variable is similar to the weights in a weighted optimization. Due to the non-linearity of the problem, a good initialization is also needed for (15). To achieve this, a RANSAC scheme was devised to provide a good initialization but also an indication of which dataset are best to use, see Algorithm 1.

In this scheme, some of the values are arbitrary and can be tuned depending on the data type etc. These values are the 5 random maps and the selection of all maps within  $1m$  of RMSE distance of the optimal anchor positions. The reason 5 maps were chosen is to maintain robustness, since the quality of maps vary, by choosing 5 maps the optimization can quickly determine a valid optimal anchor position for the majority of the iterations. The selection radius was chosen as generous catchment zone for the inlier set, this can be tuned to the specific need of the datasets.

**Algorithm 1: Our RANSAC Merging Scheme.**

- 1: Select 5 random maps
- 2: Calculate the optimal anchor positions using our merging algorithm.
- 3: **If:** The score of the objective function is the lowest value so far, select all maps within a  $1m$  of RMSE distance of the optimal anchor positions. The initial 5 maps keep their  $\lambda$  values from the optimization, all other inliers are given a value of 0.5 and outliers are given a value of 0.
- 4: Repeat steps 1-3 200 times
- 5: Recalculate a new optimal anchor position using our merging algorithm with best lambda values as an initial guess to the optimization.

## 4 EXPERIMENTAL SETUP

### 4.1 Simulated Datasets

In order to test our method, three experiments were devised. The first experiment was to create 40 anchor positions and 1000 sender positions, randomly to span a  $20 \times 20 \times 20m$  space. From there the distance matrix was calculated and Gaussian noise was added with a variance of  $0.18m$  to simulate UWB measurements. A full bundle adjustment was then performed, in order to give a comparison to current state of the art method, (Batstone et al., 2016). The distance matrix,  $d$ , was then divided into 50 equal parts of 40 anchor positions and 20 sender positions and a map was created for each set. Then for each of the 50 maps, our method was tested with different optimization methods. Firstly our linear method (13), secondly our linear method with a weighting factor (14) and lastly a bundle adjustment. This was then repeated 400 times.

The second experiment was to perform the same experiment as above but to falsify 30% and 60% of the 50 maps. For the specific percentage of the maps, the anchor positions were randomly perturbed in a  $40cm$  radius. The anchor positions were then transformed to ensure that the first anchor is the origin of the coordinate system and the second anchor on the x-axis and so on. This transformation was also performed on the sender positions. This therefore, would give a realistic poor result for those maps. The RANSAC method was then tested on these datasets to give an understanding of the robustness of the proposed merging schemes and to show how it could be used to determine good maps. Again this was repeated 400 times.

The third experiment was to test how the number of maps affects the time it takes to calculate the optimal solution. Once again, 40 anchor positions and 1000 sender positions were used like in the first experiment to simulate UWB measurements. The

RANSAC method was then used to find a solution for different number of maps, with the time it took noted, and the time for a full bundle adjustment was also noted. This was only iterated once.

### 4.2 Real Datasets

For the final experiment, our algorithms were tested on real UWB measurements from a Bitcraze, Crazyflie quadcopter mounted with a UWB device (Decawave DWM1000 chip) in order to determine if the proposed method is feasible in a real world situation, shown in Figure 1. The experiment was conducted in a Motion Capture (MOCAP) Studio to give ground truth positions to compare our results with. There were 9 separate datasets with 6 anchors in the same position for each. The ground truth anchor positions were calculated using the MOCAP cameras to a precision of  $\pm 1 mm$ .



Figure 1: Image of the Ultra-Wideband anchor and Bitcraze Crazyflie quadcopter respectively from left to right.

Distance measurements from the quadcopter to all the anchors were measured at a frequency of  $30 Hz$ .

The experiments were conducted by moving the quadcopter, by hand, around the room. The distance measurements were recorded so that they may be processed offline. Our algorithms do not require any prior knowledge of anchor or quadcopter positions. The only requirement is that the minimal solver (5,5) is satisfied for the 3D cases.

## 5 RESULTS AND ANALYSIS

### 5.1 Simulated Datasets

In Figures 2 and 3 the results for the first experiment are shown. For all the experiments the Root Mean-Squared Errors (RMSE) are a comparison of the calculated optimal anchor positions to the ground truth

anchor positions. It can be seen that each of the methods perform differently, with the linear merging scheme being the least successful. The other three methods presented show good results since all three have at least 90% of the solutions with an error under the UWB distance measurement accuracy of  $0.18m$ , see Figure 3. The full bundle adjustment result was expected to be a good solution since the optimization is minimizing the residual for all 40000 distance measurements. Interestingly, the result for the RANSAC scheme did not achieve as good a result for the best full bundle adjustment solutions but for 55% of the solutions it did achieve a better result. Furthermore, it has a steep curve at  $0.03m$  RMSE distance Error. This indicates that the method reliably produces a similar result.

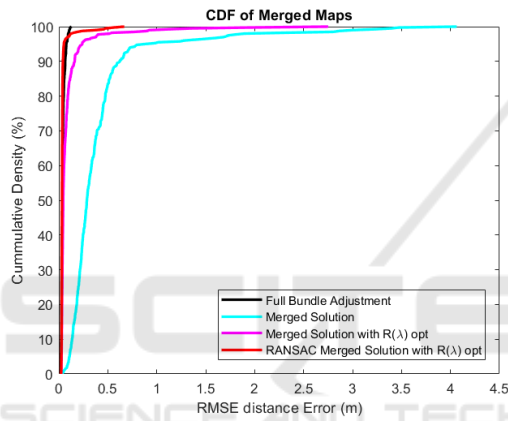


Figure 2: This figure illustrates the RMSE error for the each of the merged maps plotted against its cumulative density for 400 experiments.

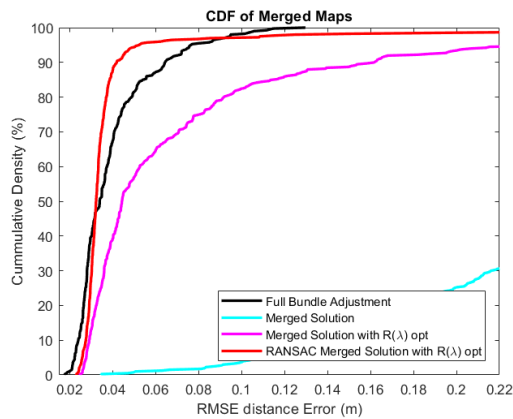


Figure 3: This figure is the same as Figure 2. It illustrates the RMSE error for the each of the merged maps plotted against its cumulative density for 400 experiments but only shows the RMSE range of 0.01 to 0.22.

In Figures 4 and 5, the results for the second experiment are shown. All three solutions show a simi-

lar result, which indicates that by using the RANSAC scheme it maintains its robustness. This is due to the RANSAC scheme being able to select a collection of maps which have similar and good results. This behaviour is further shown in Figure 5. Figure 5 is an example of the lambda values obtained after using the RANSAC scheme and the merging scheme with lambda optimization. It can be seen that the RANSAC scheme focuses the optimization of lambda in one cluster of the maps. This in turn produces better optimal anchor positions, the RANSAC scheme had a RMSE distance error of  $0.0379m$  and the merging scheme with lambda optimization  $0.0498m$ .

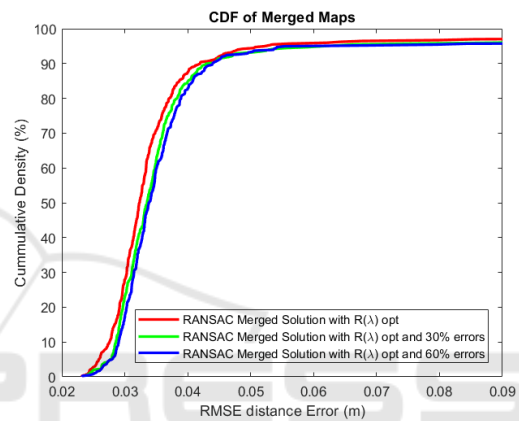


Figure 4: This figure illustrates the RMSE error for the each of the merged maps with different percentages of errors plotted against its cumulative density for 400 experiments.

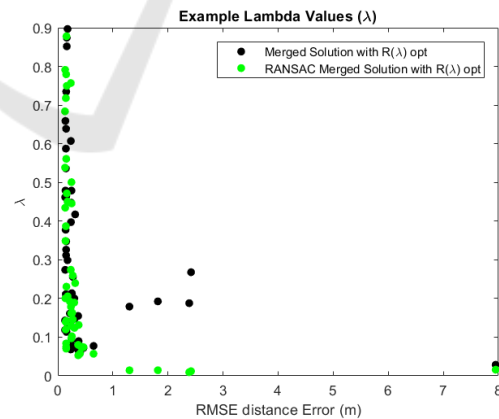


Figure 5: This figure illustrates the RMSE error for each map plotted against its calculated lambda value.

In Figure 6, the results for the third experiment is shown. It can be see that the time it takes to find a solution is dependent on the number of maps. Thus it also shows that the RANSAC method proposed is computationally cheaper. In this case, the trend appears to be parabolic which implies that there is an

optimal number of maps for each experiment. This was computed for one random experiment, the times do vary for each experiment but the trends are similar.

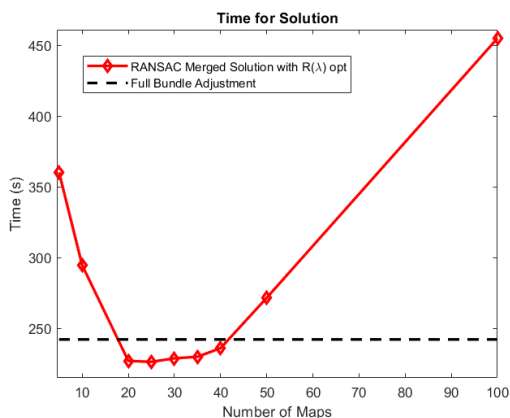


Figure 6: This figure illustrates the computational time for an optimal solution to be found for different number of maps. The time for a full Bundle Adjustment over all anchors and senders is also shown as a comparison.

## 5.2 Real Dataset

In Figure 7 are the lambda values obtained after using the RANSAC scheme and the merging scheme with lambda optimization. For this experiment the RMSE is a comparison of the calculated optimal anchor positions to the ground truth anchor positions. The RANSAC scheme had a RMSE distance error of 0.106m and the merging scheme with lambda optimization 0.1369m. Due to the restricted number of maps in this case, it is difficult to determine which of the schemes is better, since nearly all maps are needed to calculate an optimal map then the lambda value are similar.

## 6 CONCLUSIONS

In this paper, a method has been constructed to merge maps together in a linear way. In doing so we build a library of tools to determine the quality of each map, and once the quality of multiple maps were determined, we can logically merge them together to produce a global map.

Looking at the results from the MOCAP studio experiments, in Figure 7 it can be seen, that this method produces accurate results. For current Ultra-Wideband systems, the chip sets come with a recommended accuracy of  $\pm 0.2m$ . From our results, we are also able to achieve this accuracy. It is also interesting to note that the lambda values for each of the maps are

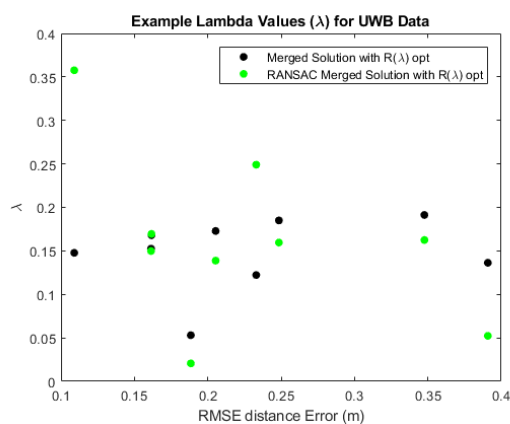


Figure 7: This figure illustrates the RMSE error for map plotted against its calculated lambda value. The maps are created using UWB mounted on a quadcopter.

varied, in particular the map with the smallest error has a lambda value of ca. 0.35. It shows potentially that there are not enough separate maps that have been collected to make a reasonable estimate of the quality of each map. One would expect the lambda values to decrease as the RMSE error increases, as seen in Figure 5, but on this occasions there are erroneous lambda values. This may be due to the non-linearity of the self-calibration problem, since there will be many local minimas, contributions from all maps may be used.

In the first experiment, our algorithms were pushed, to test the robustness of the system. From Figure 2, it can be seen that the anchor positions are calculated to a high accuracy in comparison to the full bundle adjustment. It can also be noted that roughly 98% of the merged maps had a RMSE error under 0.25m. Of course, the full bundle adjustment produces a better result and is considered the gold standard but in reality it is not a viable option. The bundle adjustment is very computationally expensive and is limited by the size of the distance matrix. During the optimization of the bundle adjustment, it has to estimate 120000 parameters (40 anchors, 1000 senders, 3 degrees of freedom), which modern computers with large RAM can calculate but any larger wouldn't be possible. By partitioning the distance matrix, multiple solutions can be created in parallel, then merged together. In addition to this, once the lambda values have been calculated, one would have an estimate of the quality of each map and the ability to logically manage each solution with data storage and merged maps quality in mind. Another benefit, is that the number of parameters is reduced considerably when performing the merging algorithm with weights. In this case from 120000 parameters to 50 parameters.

The main advantage with such linear fusion is that it is a relatively computationally cheap process, that unlocks the potential for crowd-sourced data acquisition without compromising map quality. In our case, for the simulated dataset with 60 % errors, to perform a bundle adjustment on all 50 maps and merge them took 47 minutes, whereas the full bundle adjustment took 1.5 days on the same machine for all 400 iterations. This can be seen further in Figure 6, with an appropriate number of maps. Although the computational time reduction can be seen, it is not as large as the one mentioned for the simulated dataset with 60 % errors. This may be due to the the RANSAC initialization, this step produces a robust and close initialization which reduces the time needed of our method to converge to the optimal solution. In the case for the simulated data used in experiment 3, since all the maps are viable (no outliers) then many more maps are initialized with the value 1, hence the computational time is less affected. The proposed method bridges memory requirement issues and offers the ability to select the best datasets. In addition to this, the method would also work for different media type, such as bluetooth, multiple WiFi frequencies and optical SLAM. Provided that the positions of the anchor points are the same for each media.

For future work, the study of a collaborative data management scheme would be highly advantageous. In doing so, would give an autonomous way of choosing which parts of the dataset to fuse in order to discard unnecessary data and keep only the required data to improve a map. For instance, if an office building were to be mapped using crowd-sourced data, there would exist areas that would be oversampled, such as the main entrance and corridors. Whereas a storage room would be sampled infrequently, therefore an automatic scheme that would discard the oversampled areas would be advantageous to data management. In summary, this would be a way of determining the uniqueness of a given map.

## REFERENCES

- Batstone, K., Oskarsson, M., and Åström, K. (2016). Robust time-of-arrival self calibration and indoor localization using wi-fi round-trip time measurements. In *2016 IEEE International Conference on Communications Workshops (ICC)*, pages 26–31.
- Batstone, K., Oskarsson, M., and Åström, K. (2017). Towards real-time time-of-arrival self-calibration using ultra-wideband anchors. In *2017 International Conference on Indoor Positioning and Indoor Navigation (IPIN)*, pages 1–8.
- Byröd, M. and Åström, K. (2009). *Bundle Adjustment using Conjugate Gradients with Multiscale Preconditioning*.
- Byröd, M. and Åström, K. (2010). *Conjugate Gradient Bundle Adjustment*, volume 6312, pages 114–127. Springer.
- Chanier, F., Checchin, P., Blanc, C., and Trassoudaine, L. (2008). Map fusion based on a multi-map slam framework. In *2008 IEEE International Conference on Multisensor Fusion and Integration for Intelligent Systems*, pages 533–538.
- Durrant-Whyte, H. and Bailey, T. (2006). Simultaneous localization and mapping: part i. *IEEE Robotics Automation Magazine*, 13(2):99–110.
- Jiang, F., Oskarsson, M., and Åström, K. (2015). On the minimal problems of low-rank matrix factorization. In *Proc. Conf. Computer Vision and Pattern Recognition*.
- Li, B., Salter, J., Dempster, A. G., and Rizos, C. Indoor positioning techniques based on wireless lan. In *LAN, First IEEE International Conference on Wireless Broadband and Ultra Wideband Communications*, pages 13–16.
- Liu, S., Mohta, K., Shen, S., and Kumar, V. (2016). Towards collaborative mapping and exploration using multiple micro aerial robots. In *Experimental Robotics*, pages 865–878. Springer.
- Puyol, M. G., Robertson, P., and Angermann, M. (2013). Managing large-scale mapping and localization for pedestrians using inertial sensors. In *2013 IEEE International Conference on Pervasive Computing and Communications Workshops (PERCOM Workshops)*, pages 121–126.
- Schmuck, P. and Chli, M. (2017). Multi-uav collaborative monocular slam. In *2017 IEEE International Conference on Robotics and Automation (ICRA)*, pages 3863–3870. IEEE.
- Van Opdenbosch, D., Aykut, T., Alt, N., and Steinbach, E. (2018). Efficient map compression for collaborative visual slam. In *2018 IEEE Winter Conference on Applications of Computer Vision (WACV)*, pages 992–1000. IEEE.